

# DPCL-Diff: The Temporal Knowledge Graph Reasoning based on Graph Node Diffusion Model with Dual-Domain Periodic Contrastive Learning

Yukun Cao<sup>1</sup>, Lisheng Wang<sup>2</sup>, Luobing Huang<sup>3\*</sup>†‡

## Abstract

Temporal knowledge graph (TKG) reasoning that infers future missing facts is an essential and challenging task. Predicting future events typically relies on closely related historical facts, yielding more accurate results for repetitive or periodic events. However, for future events with sparse historical interactions, the effectiveness of this method, which focuses on leveraging high-frequency historical information, diminishes. Recently, the capabilities of diffusion models in image generation have opened new opportunities for TKG reasoning. Therefore, we propose a graph node diffusion model with dual-domain periodic contrastive learning (DPCL-Diff). Graph node diffusion model (GNDiff) introduces noise into sparsely related events to simulate new events, generating high-quality data that better conforms to the actual distribution. This generative mechanism significantly enhances the model’s ability to reason about new events. Additionally, the dual-domain periodic contrastive learning (DPCL) maps periodic and non-periodic event entities to Poincaré and Euclidean spaces, leveraging their characteristics to distinguish similar periodic events effectively. Experimental results on four public datasets demonstrate that DPCL-Diff significantly outperforms state-of-the-art TKG models in event prediction, demonstrating our approach’s effectiveness. This study also investigates the combined effectiveness of GNDiff and DPCL in TKG tasks.

## 1 Introduction

Knowledge graphs (KGs) store a large amount of information about the natural world and have shown great success in many downstream applications, such as natural language processing (Hu

\*<sup>123</sup>The authors are affiliated with the School of Computer Science and Technology, Shanghai University of Electric Power (SUEP), Shanghai 201306, China

†<sup>1</sup>First author (email: marilyn\_cao@163.com)

‡<sup>2</sup>Corresponding author (email: 2207992575@mail.shiep.edu.cn)

et al., 2022; Wang et al., 2020), recommendation system (Xuan et al., 2023; Yu et al., 2022), and information retrieval (Zhou et al., 2022). Traditional KGs typically only contain static snapshots of facts, integrating facts (also known as events) in the form of static relational triples  $(s, r, o)$ , where  $s$  and  $o$  represent the subject and object entities, respectively, and  $r$  represents the relationship type. However, in the real world, knowledge evolves and constantly exhibits complex temporal dynamics (Wang et al., 2017; Yin and Cui, 2016), which has inspired the construction and application of Temporal Knowledge Graph (TKG). TKG extends the previous static relational triples  $(s, r, o)$  to quaternions  $(s, r, o, t)$  with timestamps. Thus, the TKG consists of multiple snapshots where facts in the same snapshot appear simultaneously.

Existing studies have identified two main types of new events in TKG: periodic events that will recur (Liang et al., 2023; Li et al., 2021), and events that have not occurred before but may occur in the future (Xu et al., 2023). For these new events, TKG reasoning offers fresh perspectives and insights for many downstream applications, such as event prediction (Zhou et al., 2023), political decision making (Zhang and Zhou, 2022), dialogue generation (Hou et al., 2024), and text generation (Li et al., 2022b). These applications have greatly stimulated intense interest in TKG. In this work, we focus on predicting new facts in future time, a task known as graph extrapolation (Chen et al., 2023; Li et al., 2021). Our goal is to predict the missing entities in the query  $(s, p, ?, t)$  for future timestamps  $t$  that still need to be observed in the training set.

Most current work models the structural and temporal characteristics of TKG to capture the specific relationships and temporal dependencies between different events for future event prediction. Many studies (Liang et al., 2023; Xu et al., 2023; Li et al., 2021) can predict repetitive or periodic events by

referring to the known historical events and distinguishing the different effects of periodic and non-periodic events on reasoning tasks through contrastive learning. However, in actual reasoning tasks, some periodic events share the same head entities and relations, differing only in their tail entities. This results in overly similar representations, making it difficult to distinguish them during reasoning. Additionally, In event-based TKG, new events that have never occurred account for about 40% (Jäger, 2018). Due to the sparse traces of temporal interactions throughout the timeline of these new events, it is impossible to use reasoning methods based on high-frequency periodic events, resulting in poor reasoning performance for these types of events.

To address the above problem, we propose a diffusion model-based dual-domain periodic contrast learning for timing knowledge graph reasoning (DPCL-Diff), which employs a Graph Node Diffusion model (GNDiff) to reason about new events. GNDiff tackles the issue of sparse interaction traces for new events on the timeline by introducing noise into existing correlated sparse events of the new entities. This diffusion mechanism simulates the real-world occurrence of new events and is gradually refined during the denoising process, guided by pre-trained language models (PLMs) that have been trained on extensive corpora and possess a foundational understanding of background knowledge. Consequently, this approach generates high-quality data that closely aligns with the actual distribution. The diffusion model (Ho et al., 2020; Song et al., 2020) is a cutting-edge generative framework with demonstrated powerful capabilities in both image (Ramesh et al., 2022; Rombach et al., 2022; Saharia et al., 2022) and text generation (Ou and Jian, 2024; Gong et al., 2022; Strudel et al., 2022). This provides more correlation information for inferring new events and dramatically improves the ability to reason about new events in TKG. For event inference tasks containing a large amount of temporal interaction information, we propose a novel dual-domain periodical contrast learning (DPCL) method. The periodic and non-periodic event entities related to the current event are mapped into the Poincaré and Euclidean spaces for contrastive learning, respectively. The Poincaré space property is utilized to distinguish the similar periodic event entities better.

The main contributions of this thesis are summarized below:

- We propose a TKG model called DPCL-Diff. DPCL-Diff can reason not only about periodic events but also about new events through a diffusion generation mechanism.

- GNDiff introduces a novel approach in TKG. GNDiff leverages pre-trained language models (PLMs) to conduct non-Markov decision chain-based diffusion for new events, generating high-quality data and effectively addressing the challenge of sparse interaction traces.

- We propose the DPCL method, where periodic and non-periodic event entities are mapped into the Poincaré space and Euclidean space to better distinguish similar periodic event entities.

- We conducted experiments on four public datasets. The results show that DPCL-Diff outperforms the state-of-the-art TKG model in event prediction. Additionally, we purposefully explore the effectiveness of GNDiff and DPCL in the TKG task.

## 2 Related Work

### 2.1 Diffusion Model

Diffusion models (Ho et al., 2020) are latent variable models designed for continuous data, achieving state-of-the-art sample quality in image and audio generation. To handle discrete data, prior work explored text diffusion models in discrete state spaces and defined diffusion processes for such data (Li et al., 2024; Lezama et al., 2022; Austin et al., 2021). Li et al. (2022a) focuses on continuous diffusion modelling for text, enabling gradient-based methods to control generation by introducing continuous latent representations. Ou and Jian (2024) combines discrete diffusion models with denoising techniques, significantly improving text generation quality and diversity in unconditional and conditional tasks.

### 2.2 Temporal Knowledge Graph Reasoning

TKG reasoning can be approached through interpolation or extrapolation (Chen et al., 2023; Li et al., 2021). Interpolation addresses missing events between  $t_0$  to  $t_n$ , while extrapolation predicts events beyond  $t_n$ . Interpolation models like TeAST (Li et al., 2023), Re-Temp (Wang et al., 2023), and TempCaps (Fu et al., 2022) infer missing relationships but cannot predict future events. Extrapolation methods focus on future event prediction. Know-Evolve (Trivedi et al., 2017), the first to learn nonlinear evolutionary entity embeddings, strug-

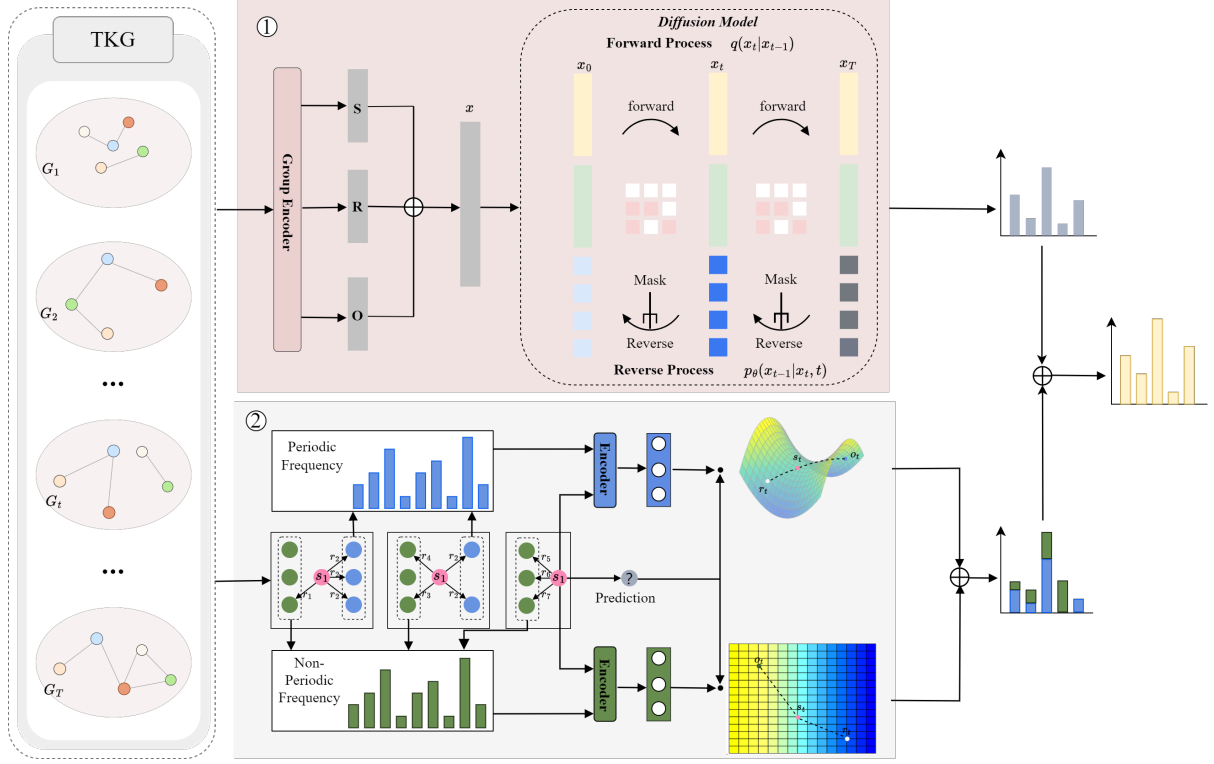


Figure 1: Overall architecture of DPCL-Diff. The first part is GNDiff, and the second part is DPCL.

gles with long-term dependencies. CyGNet (Zhu et al., 2021) uses replication generation to identify frequent repetitive events, while CENET (Xu et al., 2023) builds on this with contrastive learning to identify highly correlated entities. TARGAN (Xie et al., 2023) enhances long-term modeling using attentional mechanisms. Other models, including DynaQ (Liu et al., 2024a), EvoGNN (Pareja et al., 2020), and TempoR (Wu et al., 2020) have improved prediction but still face challenges in jointly capturing temporal evolution, semantic dependencies, and scalability.

### 3 Method

As shown in Fig. 1, for novel events, the DPCL-Diff model leverages GNDiff to inject noise into the sparse correlated events of the new event entity. This approach simulates the real-world mechanism of new events, generating numerous high-quality data samples. For other events, the DPCL method identifies highly correlated entities through comparative learning and better distinguishes similar periodic event entities using Poincaré space properties. In the following few sections, we describe our proposed approach in detail.

### 3.1 Preliminaries

TKG  $G = \{G_0, G_1, \dots, G_t, \dots, G_T\}$  is a sequence of KGs, each  $G_t = \{\mathcal{E}, \mathcal{R}, \mathcal{T}\}$  contains facts that occur at timestamp  $t$ . Let  $\mathcal{E}$ ,  $\mathcal{R}$  and  $\mathcal{T}$  denote a finite set of entities, relation types, and timestamps, respectively. Each fact is a quadruple  $(s, r, o, t)$ , where  $s \in \mathcal{E}$  is the subject entity,  $o \in \mathcal{E}$  is the object entity, and  $r \in \mathcal{R}$  is the relation at timestamp  $t$  between  $s$  and  $o$  that occurs, the dimension is  $d$ .  $\mathcal{E} \in \mathbb{R}^{|\mathcal{E}| \times d}$  is the embedding of all entities, and its rows represent the embedding vectors of an entity, such as  $s$  and  $o$ . Similarly,  $\mathcal{R} \in \mathbb{R}^{|\mathcal{R}| \times d}$  is the embedding of all relation types. The TKG inference task aims to predict missing objects by answering a query  $q = (s, r, ?, t)$  using a given history of TKG.

For a given query  $q = (s, r, ?, t)$ , we define the set of periodic events  $Q_t^{s,r}$  as the set of events that have the same head entity relationship with the query event, and the corresponding set of periodic event entities as  $\mathcal{H}_t^{s,r}$  in the following equations:

$$Q_t^{s,r} = \bigcup_{k < t} \{(s, r, o, k) \in \mathcal{G}_k\}, \quad (1)$$

$$\mathcal{H}_t^{s,r} = \{o | (s, r, o, k) \in Q_t^{s,r}\}. \quad (2)$$

Entities outside  $\mathcal{H}_t^{s,r}$  are non-periodic. If an event  $(s, r, o, t)$  does not exist in  $Q_t^{s,r}$ , it is a new

event that has never occurred and is handled by the GNDiff. For periodic event reasoning, DPCL is primarily used to predict target entities. The following sections detail these modules.

### 3.2 Graph Node Diffusion Model

In this section, we introduce GNDiff, showcasing the potential of diffusion models for TKG applications. While previous work has effectively explored the diffusion of discrete textual data, applying diffusion models to the discrete graph nodes in TKGs can be similarly effective. Traditional reasoning methods, which rely on historical data to learn implicit associations, need help to reason about new events due to the sparse historical data associated with them. In contrast, GNDiff employs a diffusion model to simulate the event generation mechanism, producing many high-quality samples for new event inference.

GNDiff consists of a forward diffusion process and a reverse diffusion process. For each quadruple  $(s, r, o, t)$ , after obtaining the vector representations of  $s$ ,  $r$ , and  $o$ , these vectors are concatenated into a single vector, which serves as the input to the graph node diffusion model. We then obtain the sample data  $x_0 \sim q(x_0)$ . Since TKGs involve discrete data, each element of  $x_t$  is a discrete random variable with  $K$  categories. For graph node,  $K = |\mathcal{V}|$  represents the number of node types. Representing  $x_t$  as a stack of heat vectors, the process of adding noise is denoted as shown in Equation 3:

$$q(x_t \mid x_{t-1}) = \text{Cat}(x_t; p = x_{t-1}Q_t), \quad (3)$$

where  $\text{Cat}(\cdot)$  denotes that the noise addition process is based on the category distribution, and  $Q_t$  is used to control the transition matrix of the node from one state to another:

$$[Q_t]_{i,j} = q(x_t = j \mid x_{t-1} = i), \quad (4)$$

The conversion relationship is shown in Equation 5:

$$\begin{aligned} q(x_{t-1} \mid x_t, x_0) &= \frac{q(x_t \mid x_{t-1}, x_0)q(x_{t-1} \mid x_0)}{q(x_t \mid x_0)} \\ &= \text{Cat}\left(x_{t-1}; p = \frac{x_t Q_t^\top \odot x_0 \bar{Q}_{t-1}}{x_0 \bar{Q}_t x_t^\top}\right), \end{aligned} \quad (5)$$

where  $\bar{Q}_t = Q_1 Q_2 \cdots Q_t$ . Note that  $\odot$  denotes elementwise multiplication, and division is performed rowwise. To be combined with pre-trained denoising language models, we incorporate an absorbing

state, allowing for the generation of samples during denoising. We use the masking mechanism to simulate the possible inactive state of the node. The transition matrix adjustment process is shown in Equation 6:

$$[Q_t]_{i,j} = \begin{cases} 1 & \text{if } i = j = [\text{M}], \\ \beta_t & \text{if } j = [\text{M}], i \neq [\text{M}], \\ 1 - \beta_t & \text{if } i = j \neq [\text{M}], \end{cases} \quad (6)$$

Here,  $[\text{M}]$  denotes a node in a masked state (an inactive node), allowing nodes to transition naturally in and out of this state as the graph evolves, eventually converging to a smooth distribution  $q(x_T)$ . This approach concentrates all probability mass on a sequence labelled with a mask. By using  $\bar{Q}_t = Q_1 Q_2 \cdots Q_t$ , the transfer relation for multiple time steps can be derived. Samples are then generated through a backward diffusion process:

$$p_\theta(x_{0:T}) = p(x_T) \prod_{t=1}^T p_\theta(x_{t-1} \mid x_t, t), \quad (7)$$

We optimize the inverse process by minimizing the variational lower bound to maximize the log-likelihood of the original data. This approach derives the optimization objective  $p_\theta(x_{0:T})$  and controls the optimization through  $\mathcal{L}_{\text{diff}}$ :

$$\begin{aligned} \mathcal{L}_{\text{diff}} &= \mathbb{E}_q[\text{D}_{\text{KL}}(q(x_T \mid x_0) \parallel p_\theta(x_T))] + \\ &\mathbb{E}_q\left[\sum_{t=2}^T \text{D}_{\text{KL}}(q(x_{t-1} \mid x_t, x_0) \parallel p_\theta(x_{t-1} \mid x_t, t))\right] \\ &- \log p_\theta(x_0 \mid x_1), \end{aligned} \quad (8)$$

where  $\mathbb{E}_q$  denotes the expectation under a noisy data distribution.  $\text{D}_{\text{KL}}$  stands for Kullback-Leibler divergence.

### 3.3 Dual-Domain Periodic Contrastive Learning

Inspired by Xu et al. (2023), we propose a dual-domain periodic contrastive learning method. Unlike the original approach, we use a dual-domain mapping strategy because we observed that specific queries involve multiple similar periodic events that are challenging to distinguish. To address this issue, we map entities from periodic and non-periodic events to Poincaré and Euclidean space, respectively, to identify highly correlated entities within each domain. By leveraging the spatial characteristics of Poincaré space, we effectively differentiate similar periodic entities.

During data preprocessing, we analyze entity frequencies for a given query  $q = (s, r, ?, t)$ , as shown in Equation 13:

$$\mathbf{Z}_t^{s,r}(o) = \lambda \cdot (\Phi_{\beta>0} - \Phi_{\beta=0}), \quad (9)$$

$$\beta = \sum_{(s,r,o_i,k) \in G_k} (o_i = o), \quad (10)$$

where the value of each entity frequency is constrained by the hyperparameter  $\lambda$ .  $\Phi_\beta$  is an indicator function that returns 1 if  $\beta$  is true and 0 otherwise.  $\mathbf{Z}_t^{s,r}(o) > 0$  indicates that quadruple  $(s, r, o, t_k)$  is a periodic event bound to  $s$  and  $r$ ; otherwise, it is a non-periodic event. DPCL then learns dependencies in periodic and non-periodic events based on the input  $\mathbf{Z}_t^{s,r}(o)$ . The distance between entities in Poincaré space is used as the final similarity score between an entity  $o_i \in \mathcal{E}$  and a query  $q$ . The formula for calculating the Poincaré distance is provided as follows:

$$\mathbf{S}_p^{s,r}(o_i) = \tanh(\mathbf{W}_p s \oplus r + \mathbf{b}_p) \mathbf{E}^T + \mathbf{Z}_t^{s,r} + \mathbf{d}_p(s, o_i), \quad (11)$$

where  $\mathbf{S}_p^{s,r}$  denotes the periodic dependency score for different object entities,  $\tanh$  is the activation function,  $\oplus$  denotes the connection operator, and  $\mathbf{W}_p \in R^{d \times 2d}$ ,  $\mathbf{b}_p \in R^{d \times 2d}$  are the trainable parameters. We compute the initial similarity score between each entity  $o_i \in E$  and the query  $q$  using a linear layer with activation.

For non-periodic dependencies, we calculate the similarity scores  $d_E(s, o) = \|s - o\|$  using the following Euclidean distance formula to obtain the non-periodic dependency score  $\mathbf{S}_{np}^{s,r}$ :

$$\mathbf{S}_{np}^{s,r}(o_i) = \tanh(\mathbf{W}_{np} s \oplus r + \mathbf{b}_{np}) \mathbf{E}^T - \mathbf{Z}_t^{s,r} + d_E(s, o_i), \quad (12)$$

The training objective of learning from periodic and non-periodic events is to minimize the loss  $\mathcal{L}_{ce}$ :

$$\mathcal{L}_{ce} = - \sum_q \log \left\{ \frac{\exp(\mathbf{S}_p^{s,r}(o_i))}{\sum_j \exp(\mathbf{S}_p^{s,r}(o_j))} + \frac{\exp(\mathbf{S}_{np}^{s,r}(o_i))}{\sum_j \exp(\mathbf{S}_{np}^{s,r}(o_j))} \right\} \quad (13)$$

where  $o_i$  denotes the ground truth object entity for a given query  $q$ . The goal of  $\mathcal{L}_{ce}$  is to distinguish the ground truth from other values by comparing each scalar in  $\mathbf{S}_p^{s,r}$  and  $\mathbf{S}_{np}^{s,r}$ .

The model employs supervised contrastive learning to enhance its discriminative power by enforcing consistency within the same class and differentiation between different classes, controlled by the

supervised contrastive loss  $\mathcal{L}_{sup}$ :

$$\mathcal{L}_{sup} = \sum_{q \in I} \frac{-1}{|P(i)|} \sum_{p \in P(i)} \log \frac{\exp(z_q \cdot z_p / \tau)}{\sum_a \exp(z_q \cdot z_a / \tau)}. \quad (14)$$

where  $\tau$  is the temperature parameter set to 0.1 in experiments,  $I$  is the set of positive samples,  $P(i)$  is the set of queries with the same label in the small batch,  $z_q$  denotes the embedding vector of query  $q$ ,  $z_p$  represents the embedding vector of queries sharing the same label as  $q$ ,  $z_a$  denotes the embedding vector of all non- $q$  queries in the small batch.

DPCL-Diff will choose the object with the highest probability as the final prediction  $o_i$ .

### 3.4 Training Details and Inference

DPCL-Diff minimizes the loss function throughout model training:

$$\mathcal{L}_{dpcl} = \alpha \cdot \mathcal{L}_{diff} + (1 - \alpha) \cdot (\mathcal{L}_{ce} + \mathcal{L}_{sup}), \quad (15)$$

where  $\alpha$  is the equilibrium coefficient.

In GNDiff, the inference process closely mirrors the generation process, so candidate entity probability is computed via reverse diffusion.

$$\mathbf{P}_{diff}(o_i | q) = \prod_{t=1}^T p_\theta(x_{t-1} | x_t), \quad (16)$$

where  $o_i$  is the tail entity representation in the generated sample  $x_t$ , and  $x_t$  represents the sample corresponding to the query  $q$ .

For DPCL the probability distribution of entities is calculated based on the predicted missing objects:

$$\mathbf{P}_{dpcl}(o_i | q) = \frac{\exp(s(o_i | q))}{\sum_{o_j \in \mathcal{E}} \exp(s(o_j | q))}, \quad (17)$$

The final probability  $\mathbf{P}(o_i)$  is obtained by averaging the probabilities from the diffusion process and the DPCL prediction:

$$\mathbf{P}(o_i | q) = \frac{1}{2} (\mathbf{P}_{diff}(o_i | q) + \mathbf{P}_{dpcl}(o_i | q)). \quad (18)$$

## 4 Experiments

### 4.1 Experimental Setup

**Datasets and Evaluation Metrics.** To evaluate the effectiveness of the proposed DPCL-Diff, we report the reasoning performance on four public datasets:

Method	ICEWS18				ICEWS14			
	MRR	Hits@1	Hits@3	Hits@10	MRR	Hits@1	Hits@3	Hits@10
ComplEx(2016)	30.09	21.88	34.15	45.96	24.47	16.13	27.49	41.09
R-GCN(2018)	23.19	16.36	25.34	36.48	26.31	18.23	30.43	45.34
ConvE(2018)	36.67	28.51	39.80	50.69	40.73	33.20	43.92	54.35
RE-Net(2019)	42.93	36.19	45.47	55.80	45.71	38.42	49.06	59.12
xERTE(2020)	36.95	30.71	40.38	49.76	32.92	26.44	36.58	46.05
CyGNet(2021)	17.21	30.97	46.85	27.12	27.43	42.63	57.90	37.65
EvoKG(2022)	29.67	12.92	33.08	<u>58.32</u>	18.30	6.30	19.43	39.37
RPC(2023)	34.91	24.34	38.74	55.89	44.55	34.87	49.80	65.08
CENET(2023)	43.72	37.91	45.65	54.79	<u>51.93</u>	<u>48.24</u>	<u>52.81</u>	59.33
DHE-TKG(2024)	29.23	19.15	33.31	—	40.02	30.13	44.99	—
RLGNet(2024)	29.90	20.18	33.64	49.08	39.06	29.34	42.03	58.12
HisRES(2024)	37.69	26.46	42.75	59.70	50.48	39.57	<u>56.65</u>	<u>71.09</u>
DiffuTKG(2024)	36.72	25.73	—	57.81	48.51	36.41	—	<u>72.75</u>
DPCL-Diff	<b>47.02</b>	40.03	<b>49.93</b>	<b>60.66</b>	<b>66.59</b>	<b>62.89</b>	<b>67.79</b>	<b>73.64</b>

Table 1: TKG entity extrapolation results on four datasets. The time-filtered MRR, H@1, H@3, and H@10 metrics are multiplied by 100. The best results are in bold, and the previous best results are underlined.

ICEWS14 (Trivedi et al., 2017), ICEWS18 (Jin et al., 2019), WIKI (Leblay and Chekol, 2018), and YAGO (Mahdisoltani et al., 2013). Table 3 shows more detailed information about the datasets. We divided all datasets into three groups, roughly partitioning them into train (80%), validation (10%), and test (10%) sets by timestamp. In our experiments, we chose the mean reversed rank (MRR) and the hit rate @1,3,10 (Liang et al., 2023) as the metrics.

**Baselines.** DPCL-Diff is compared with both static and temporal KG reasoning models. Static KG reasoning models, which do not consider temporal information, include ComplEx (Trouillon et al., 2016), R-GCN (Schlichtkrull et al., 2018) and ConvE (Dettmers et al., 2018). In contrast, temporal KG reasoning models are designed to process temporal information and capture evolving patterns in TKG, such as RE-Net (Jin et al., 2019), xERTE (Z et al., 2020), CyGNet (Zhu et al., 2021), EvoKG (Park et al., 2022), RPC (Liang et al., 2023), CENET (Xu et al., 2023), DHE-TKG (Liu et al., 2024b), RLGNet (Lv et al., 2024), and DiffuTKG (Cai et al., 2024).

**Implementation Details.** For all datasets, the initial embedding dimension is configured as 200. We set the batch size to 64, the embedding dimension to 200, and the learning rate to 0.001, and we used the Adam optimizer. The training calendar element limit for L is 30, and the comparison learning calendar element limit for the second stage is 20.

For baseline settings, we use their recommended configuration. All experiments were implemented on servers with RTX 3090 GPUs equipped with Intel Xeon Gold 6330 CPUs.

## 4.2 Main Results

We compared the experimental results in Table 1 and Table 2, which provides the MRR and Hits@1/3/10 metrics of DPCL-Diff on four datasets. DPCL-Diff outperforms 13 other comparison models in most cases, particularly excelling on ICEWS14, where it achieves a 29.54% improvement in Hits@1 over our baseline model CENET. This significant gain is mainly due to effective data generation techniques, enabling the model to handle unseen events more effectively. ICEWS14 has a high proportion of new events (about 30% (Xu et al., 2023)) and contains the most significant volume of data among the four datasets. DPCL-Diff generates substantial-high-quality data through GNDiff, enhancing inference on these events and improving overall performance. / Moreover, while DiffuTKG was the first to introduce diffusion processes in TKG inference, DPCL-Diff further leverages a pre-trained language model (PLM) in the denoising process, capturing contextual information more effectively and aligning data generation closer to actual event distributions. This is particularly advantageous in scenarios with sparse interaction trajectories, leading to superior predictive accuracy and allowing DPCL-Diff to outperform DiffuTKG

Method	WIKI				YAGO			
	MRR	Hits@1	Hits@3	Hits@10	MRR	Hits@1	Hits@3	Hits@10
ComplEx(2016)	47.84	38.15	50.08	58.46	61.29	54.88	62.28	69.42
R-GCN(2018)	37.57	28.15	39.66	—	41.3	32.56	44.44	—
ConvE(2018)	47.57	38.76	50.1	63.74	62.32	56.19	63.97	70.44
RE-Net(2019)	51.97	48.01	52.07	53.91	65.16	63.29	65.63	68.08
xERTE(2020)	58.75	58.46	58.85	59.34	58.75	58.46	58.85	60.48
CyGNet(2021)	47.89	66.44	78.70	58.78	17.21	30.97	46.85	27.12
EvoKG(2022)	50.66	12.21	63.84	64.73	55.11	54.37	81.38	92.73
CENET(2023)	66.87	66.77	66.93	66.98	79.64	78.65	79.91	81.42
DHE-TKG(2024)	51.20	57.47	69.25	—	62.93	71.00	82.72	—
RLGNet(2024)	64.34	61.03	66.71	<b>69.51</b>	80.17	76.52	83.57	<b>84.96</b>
DPCL-Diff	<b>68.44</b>	<b>68.41</b>	<b>68.45</b>	68.55	<b>84.45</b>	<b>84.23</b>	<b>84.65</b>	84.75

Table 2: Experimental results of temporal link prediction on two public KGs.

Dataset	#Ent	#Re	#Train	#Valid	#Test
ICEWS18	23,033	256	373,018	45,995	49,545
ICEWS14	12,498	260	535,654	63,788	65,861
WIKI	12,554	24	539,286	67,538	63,110
YAGO	10,623	10	161,540	19,523	20,026

Table 3: Statistics of the datasets.

across key metrics, especially in datasets with a high proportion of new events./ For the YAGO and WIKI datasets, DPCL-Diff also outperforms other algorithms on most metrics, except for Hits@10 on YAGO, which is slightly lower than RLGNet but significantly higher in Hits@1. DPCL-Diff ability to distinguish similar periodic event entities improves prediction accuracy. Although YAGO and WIKI have a lower proportion of new events (about 10% (Xu et al., 2023)) and a higher percentage of periodic events, which limits GNDiff performance, DPCL-Given that the GNDiff parameters used in this experiment are relatively low, with the batch size set to 64, these settings may influence the results. We believe the performance could be significantly improved if the batch size is increased to 512 or 1024.

### 4.3 Ablation Study

To investigate the effectiveness of the modules in DPCL-Diff, we verified the effectiveness of GNDiff and DPCL through ablation experiments. The ablation results are shown in Table 4. Here, "w/o GNDiff" denotes the removal of the graph node diffusion model, and "w/o-DPCL" denotes the removal of the Poincaré mapping, which maps both

positive and negative samples into the Euclidean space for contrast learning. These results illustrate the effectiveness of our proposed GNDiff and DPCL. The performance degradation is particularly noticeable after the removal of GNDiff. This demonstrates that generating a large number of high-quality data related to the predicted event through GNDiff significantly affects event prediction. DPCL leverages Poincaré space properties to distinguish similar periodic events better, enhancing inference accuracy.

### 4.4 Dual Domain Mapping Strategy Analysis

In this study, we separately examined the effects of different spatial mapping strategies on the learning effect of DPCL. Table 4 shows the results of the experiments on the YAGO dataset without the GNDiff. Euc/Hyp denotes that periodic and non-periodic event entities are mapped to Euclidean and Poincaré spaces respectively for comparative learning, Hyp/ Euc denotes that the two types of entities are mapped to Poincaré and Euclidean space, Hyp/Hyp denotes that both types of entities are mapped to Poincaré space, and Euc / Euc denotes that the two types of entities are mapped to Euclidean space respectively. From the experimental results, it can be seen that the Hyp/Euc method is the most effective, while the Euc/Euc method is the least effective. This suggests that mapping periodic and non-periodic event entities to separate spaces can improve the modeling of comparative learning. Specifically, the geometric properties of the Poincaré space can effectively distinguish entities whose feature representations are too close to each other in the Euclidean space.

Method	YAGO				ICEWS18			
	MRR	Hits@1	Hits@5	Hits@10	MRR	Hits@1	Hits@5	Hits@10
w/o- GNDif	81.30	80.64	81.42	82.26	44.93	38.22	47.53	57.08
w/o- DPCL	84.21	84.19	84.23	84.34	46.51	39.92	48.92	59.67
<b>DPCL-Diff</b>	<b>84.45</b>	<b>84.23</b>	<b>84.65</b>	<b>84.75</b>	<b>47.02</b>	<b>40.03</b>	<b>49.93</b>	<b>60.66</b>

Table 4: DPCL-Diff ablation studies on YAGO and ICEWS18 datasets.

Method	YAGO			
	MRR	Hits@1	Hits@5	Hits@10
Euc/Hyp	81.20	80.60	81.26	82.08
Hyp/Hyp	81.23	80.62	81.30	82.14
Euc/Euc	79.64	78.65	79.91	81.42
<b>Hyp/Euc</b>	<b>81.30</b>	<b>80.64</b>	<b>81.42</b>	<b>82.26</b>

Table 5: Experimental results of DPCL under different spatial mapping strategies

## 5 Conclusion

In this paper, we propose a temporal knowledge graph inference method based on a graph node diffusion model with dual-domain periodic contrastive learning. This method aims to alleviate the prediction difficulties caused by the limited interactions of new events on the timeline. We enhance new event reasoning by generating graph data through graph node diffusion, where noise is introduced and adjusted to simulate real-world event mechanisms, producing samples that better reflect actual distributions. Additionally, the performance of the temporal knowledge reasoning task is enhanced by mapping event entities to Poincaré space and Euclidean space through dual-domain periodic contrastive learning, effectively distinguishing between periodic and non-periodic events. Extensive experiments demonstrate the reasoning advantages and effectiveness of DPCL-Diff on public temporal knowledge graph datasets.

## 6 Limitations

This study does not incorporate adaptive embedding strategies to distinguish between periodic and non-periodic events. Consequently, our approach lacks the flexibility to dynamically adjust to different types of temporal knowledge graph data. This limitation could potentially impact the model’s effectiveness when applied to datasets with varying temporal characteristics.

## References

Jacob Austin, Daniel D Johnson, Jonathan Ho, Daniel Tarlow, and Rianne Van Den Berg. 2021. Structured denoising diffusion models in discrete state-spaces. *Advances in Neural Information Processing Systems*, 34:17981–17993.

Yuxiang Cai, Qiao Liu, Yanglei Gan, Changlin Li, Xueyi Liu, Run Lin, Da Luo, and Jiaye Yang Jiaye Yang. 2024. Predicting the unpredictable: Uncertainty-aware reasoning over temporal knowledge graphs via diffusion process. In *Findings of the Association for Computational Linguistics ACL 2024*, pages 5766–5778.

Zhongwu Chen, Chengjin Xu, Fenglong Su, Zhen Huang, and Yong Dou. 2023. Temporal extrapolation and knowledge transfer for lifelong temporal knowledge graph reasoning. In *Findings of the Association for Computational Linguistics: EMNLP 2023*, pages 6736–6746.

Tim Dettmers, Pasquale Minervini, Pontus Stenetorp, and Sebastian Riedel. 2018. Convolutional 2d knowledge graph embeddings. In *Proceedings of the AAAI conference on artificial intelligence*, volume 32.

Guirong Fu, Zhao Meng, Zhen Han, Zifeng Ding, Yunpu Ma, Matthias Schubert, Volker Tresp, and Roger Wattenhofer. 2022. Tempcaps: a capsule network-based embedding model for temporal knowledge graph completion. In *Proceedings of the Sixth Workshop on Structured Prediction for NLP*, pages 22–31. Association for Computational Linguistics.

Shanshan Gong, Mukai Li, Jiangtao Feng, Zhiyong Wu, and LingPeng Kong. 2022. Diffuseq: Sequence to sequence text generation with diffusion models. *arXiv preprint arXiv:2210.08933*.

Jonathan Ho, Ajay Jain, and Pieter Abbeel. 2020. Denoising diffusion probabilistic models. *Advances in neural information processing systems*, 33:6840–6851.

Zhongni Hou, Xiaolong Jin, Zixuan Li, Long Bai, Jiafeng Guo, and Xueqi Cheng. 2024. Selective temporal knowledge graph reasoning. *arXiv preprint arXiv:2404.01695*.

Ziniu Hu, Yichong Xu, Wenhao Yu, Shuohang Wang, Ziyi Yang, Chenguang Zhu, Kai-Wei Chang, and Yizhou Sun. 2022. Empowering language models

with knowledge graph reasoning for question answering. *arXiv preprint arXiv:2211.08380*.

Kai Jäger. 2018. The limits of studying networks via event data: Evidence from the icews dataset. *Journal of Global Security Studies*, 3(4):498–511.

Woojeong Jin, Meng Qu, Xisen Jin, and Xiang Ren. 2019. Recurrent event network: Autoregressive structure inference over temporal knowledge graphs. *arXiv preprint arXiv:1904.05530*.

Julien Leblay and Melisachew Wudage Chekol. 2018. Deriving validity time in knowledge graph. In *Companion proceedings of the the web conference 2018*, pages 1771–1776.

Jose Lezama, Tim Salimans, Lu Jiang, Huiwen Chang, Jonathan Ho, and Irfan Essa. 2022. Discrete predictor-corrector diffusion models for image synthesis. In *The Eleventh International Conference on Learning Representations*.

Bocheng Li, Zhujin Gao, Yongxin Zhu, Kun Yin, Haoyu Cao, Deqiang Jiang, and Linli Xu. 2024. Few-shot temporal pruning accelerates diffusion models for text generation. In *Proceedings of the 2024 Joint International Conference on Computational Linguistics, Language Resources and Evaluation (LREC-COLING 2024)*, pages 7259–7269.

Jiang Li, Xiangdong Su, and Guanglai Gao. 2023. Teast: Temporal knowledge graph embedding via archimedean spiral timeline. In *Proceedings of the 61st Annual Meeting of the Association for Computational Linguistics (Volume 1: Long Papers)*, pages 15460–15474.

Xiang Li, John Thickstun, Ishaan Gulrajani, Percy S Liang, and Tatsunori B Hashimoto. 2022a. Diffusion-Im improves controllable text generation. *Advances in Neural Information Processing Systems*, 35:4328–4343.

Zixuan Li, Saiping Guan, Xiaolong Jin, Weihua Peng, Yajuan Lyu, Yong Zhu, Long Bai, Wei Li, Jiafeng Guo, and Xueqi Cheng. 2022b. Complex evolutional pattern learning for temporal knowledge graph reasoning. *arXiv preprint arXiv:2203.07782*.

Zixuan Li, Xiaolong Jin, Wei Li, Saiping Guan, Jiafeng Guo, Huawei Shen, Yuanzhuo Wang, and Xueqi Cheng. 2021. Temporal knowledge graph reasoning based on evolutional representation learning. In *Proceedings of the 44th international ACM SIGIR conference on research and development in information retrieval*, pages 408–417.

Ke Liang, Lingyuan Meng, Meng Liu, Yue Liu, Wenxuan Tu, Siwei Wang, Sihang Zhou, and Xinwang Liu. 2023. Learn from relational correlations and periodic events for temporal knowledge graph reasoning. In *Proceedings of the 46th international ACM SIGIR conference on research and development in information retrieval*, pages 1559–1568.

Ruinan Liu, Guisheng Yin, Zechao Liu, and Ye Tian. 2024a. Reinforcement learning with time intervals for temporal knowledge graph reasoning. *Information Systems*, 120:102292.

Xinyue Liu, Jianan Zhang, Chi Ma, Wenxin Liang, Bo Xu, and Linlin Zong. 2024b. Temporal knowledge graph reasoning with dynamic hypergraph embedding. In *Proceedings of the 2024 Joint International Conference on Computational Linguistics, Language Resources and Evaluation (LREC-COLING 2024)*, pages 15742–15751.

Ao Lv, Yongzhong Huang, Guige Ouyang, Yue Chen, and Haoran Xie. 2024. Rlgnnet: Repeating-local-global history network for temporal knowledge graph reasoning. *arXiv preprint arXiv:2404.00586*.

Farzaneh Mahdisoltani, Joanna Biega, and Fabian M Suchanek. 2013. Yago3: A knowledge base from multilingual wikipedias. In *CIDR*.

Yimin Ou and Ping Jian. 2024. Effective integration of text diffusion and pre-trained language models with linguistic easy-first schedule. In *Proceedings of the 2024 Joint International Conference on Computational Linguistics, Language Resources and Evaluation (LREC-COLING 2024)*, pages 5551–5561.

Aldo Pareja, Giacomo Domeniconi, Jie Chen, Tengfei Ma, Toyotaro Suzumura, Hiroki Kanezashi, Tim Kaler, Tao Schardl, and Charles Leiserson. 2020. Evolvegen: Evolving graph convolutional networks for dynamic graphs. In *Proceedings of the AAAI conference on artificial intelligence*, volume 34, pages 5363–5370.

Namyong Park, Fuchen Liu, Purvanshi Mehta, Dana Cristofor, Christos Faloutsos, and Yuxiao Dong. 2022. Evokg: Jointly modeling event time and network structure for reasoning over temporal knowledge graphs. In *Proceedings of the fifteenth ACM international conference on web search and data mining*, pages 794–803.

Aditya Ramesh, Prafulla Dhariwal, Alex Nichol, Casey Chu, and Mark Chen. 2022. Hierarchical text-conditional image generation with clip latents. *arXiv preprint arXiv:2204.06125*, 1(2):3.

Robin Rombach, Andreas Blattmann, Dominik Lorenz, Patrick Esser, and Björn Ommer. 2022. High-resolution image synthesis with latent diffusion models. In *Proceedings of the IEEE/CVF conference on computer vision and pattern recognition*, pages 10684–10695.

Chitwan Saharia, William Chan, Saurabh Saxena, Lala Li, Jay Whang, Emily L Denton, Kamayyar Ghasemipour, Raphael Gontijo Lopes, Burcu Karagol Ayan, Tim Salimans, et al. 2022. Photorealistic text-to-image diffusion models with deep language understanding. *Advances in neural information processing systems*, 35:36479–36494.

Michael Schlichtkrull, Thomas N Kipf, Peter Bloem, Rianne Van Den Berg, Ivan Titov, and Max Welling. 2018. Modeling relational data with graph convolutional networks. In *The semantic web: 15th international conference, ESWC 2018, Heraklion, Crete, Greece, June 3–7, 2018, proceedings 15*, pages 593–607. Springer.

Jiaming Song, Chenlin Meng, and Stefano Ermon. 2020. Denoising diffusion implicit models. *arXiv preprint arXiv:2010.02502*.

Robin Strudel, Corentin Tallec, Florent Altché, Yilun Du, Yaroslav Ganin, Arthur Mensch, Will Grathwohl, Nikolay Savinov, Sander Dieleman, Laurent Sifre, et al. 2022. Self-conditioned embedding diffusion for text generation. *arXiv preprint arXiv:2211.04236*.

Rakshit Trivedi, Hanjun Dai, Yichen Wang, and Le Song. 2017. Know-evolve: Deep temporal reasoning for dynamic knowledge graphs. In *international conference on machine learning*, pages 3462–3471. PMLR.

Théo Trouillon, Johannes Welbl, Sebastian Riedel, Éric Gaussier, and Guillaume Bouchard. 2016. Complex embeddings for simple link prediction. In *International conference on machine learning*, pages 2071–2080. PMLR.

Kunze Wang, Soyeon Caren Han, and Josiah Poon. 2023. Re-temp: Relation-aware temporal representation learning for temporal knowledge graph completion. *arXiv preprint arXiv:2310.15722*.

Qingyun Wang, Manling Li, Xuan Wang, Nikolaus Parulian, Guangxing Han, Jiawei Ma, Jingxuan Tu, Ying Lin, Haoran Zhang, Weili Liu, et al. 2020. Covid-19 literature knowledge graph construction and drug repurposing report generation. *arXiv preprint arXiv:2007.00576*.

Quan Wang, Zhendong Mao, Bin Wang, and Li Guo. 2017. Knowledge graph embedding: A survey of approaches and applications. *IEEE transactions on knowledge and data engineering*, 29(12):2724–2743.

Jiapeng Wu, Meng Cao, Jackie Chi Kit Cheung, and William L Hamilton. 2020. Temp: Temporal message passing for temporal knowledge graph completion. *arXiv preprint arXiv:2010.03526*.

Zhiwen Xie, Runjie Zhu, Jin Liu, Guangyou Zhou, and Jimmy Xiangji Huang. 2023. Targat: A time-aware relational graph attention model for temporal knowledge graph embedding. *IEEE/ACM Transactions on Audio, Speech, and Language Processing*, 31:2246–2258.

Yi Xu, Junjie Ou, Hui Xu, and Luoyi Fu. 2023. Temporal knowledge graph reasoning with historical contrastive learning. In *Proceedings of the AAAI Conference on Artificial Intelligence*, volume 37, pages 4765–4773.

Hongrui Xuan, Yi Liu, Bohan Li, and Hongzhi Yin. 2023. Knowledge enhancement for contrastive multi-behavior recommendation. In *Proceedings of the sixteenth ACM international conference on web search and data mining*, pages 195–203.

Hongzhi Yin and Bin Cui. 2016. *Spatio-temporal recommendation in social media*. Springer.

Junliang Yu, Hongzhi Yin, Xin Xia, Tong Chen, Lizhen Cui, and Quoc Viet Hung Nguyen. 2022. Are graph augmentations necessary? simple graph contrastive learning for recommendation. In *Proceedings of the 45th international ACM SIGIR conference on research and development in information retrieval*, pages 1294–1303.

Han Z, Chen P., Ma Y., and Tresp V. 2020. Explainable subgraph reasoning for forecasting on temporal knowledge graphs. In *International Conference on Learning Representations*.

Linhai Zhang and Deyu Zhou. 2022. Temporal knowledge graph completion with approximated gaussian process embedding. In *Proceedings of the 29th International Conference on Computational Linguistics*, pages 4697–4706.

Wang-Tao Zhou, Zhao Kang, Ling Tian, and Yi Su. 2023. Intensity-free convolutional temporal point process: Incorporating local and global event contexts. *Information Sciences*, 646:119318.

Ying Zhou, Xuanang Chen, Ben He, Zheng Ye, and Le Sun. 2022. Re-thinking knowledge graph completion evaluation from an information retrieval perspective. In *Proceedings of the 45th International ACM SIGIR Conference on Research and Development in Information Retrieval*, pages 916–926.

Cunchao Zhu, Muhan Chen, Changjun Fan, Guangquan Cheng, and Yan Zhang. 2021. Learning from history: Modeling temporal knowledge graphs with sequential copy-generation networks. In *Proceedings of the AAAI conference on artificial intelligence*, volume 35, pages 4732–4740.

## Appendices

## 7 Extended Experiments

### 7.1 Dual Domain embedded visual analytics

In this section, we investigate the visualization of entities in DPCL with bi-domain embedding. As shown in Fig. 2, we visualize two sets of entity pairs—(Germany, Berlin) and (Germany, Munich)—with the same relation, mapping them to Euclidean and Poincaré space, respectively. In Euclidean space, due to the similar Euclidean distance between Berlin and Munich to Germany, it is difficult to distinguish between these two entities effectively. However, in Poincaré space, Germany is significantly farther from Munich, bringing Germany

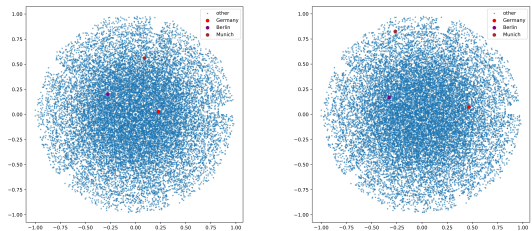


Figure 2: Illustration of 2D entity embedding learned by Euc (left) and Hyp (right) on YAGO.

closer to Berlin and making it easier to derive the correct inference. By leveraging the spatial properties of Poincaré space, we can more effectively distinguish similar periodic event entities and improve the overall prediction accuracy of the model.